Available online at www.sciencedirect.com

ScienceDirect

Energy Procedia 45 (2014) 749 – 758

Energy Procedia

68th Conference of the Italian Thermal Machines Engineering Association, ATI2013

Influence of the Diesel injector hole geometry on the flow conditions emerging from the nozzle

Federico Brusiani[a]*, Stefania Falfari[a], Piero Pelloni[a]

[a]*Department DIN, University of Bologna, Bologna, 40136, Italy*

Abstract

Engine performances are correlated to the overall fluid dynamic characteristics of the injection system that, in turns, are strictly correlated to the fluid dynamic performance of the injector geometry. It is particularly true for actual GDI and Diesel engines where micro-orifice configurations are associated to very high injection pressure.
In relation to the Common Rail Diesel engines, over the last decade different injector hole shapes have been tested. Actually, the most used configurations are: cylindrical, *k*, and *ks*. In this paper, the performance of all these three injector hole shapes are evaluated in order to find out the influence of orifice conicity and hydro-grinding level on the main fluid dynamic characteristics like cavitation evolution inside the injector as well as the flow properties at nozzle exit. The fluid dynamic behavior of each considered hole is evaluated over the injection time by performing a fully transient CFD multiphase simulation (i.e. the needle motion is reproduced during the simulation). By the proposed simulation methodology, the evaluation of the cavitating flow evolution inside the injector is performed not only from the point of view of the overall spray characteristics emerging from the injector holes but also from the cavitation erosion risk over needle, nozzle, and hole internal surfaces.

Keywords: Common Rail; Injection system; Cavitation;

* Corresponding author. Tel.: +39-051-209.3314; fax: +39-051-209.3313.
E-mail address: federico.brusiani3@unibo.it

doi:10.1016/j.egypro.2014.01.080

1. Introduction

In modern Diesel engines, the combustion efficiency is strongly correlated to the spray behaviour. In turns, as showed by many studies [1-9] the main spray characteristics (atomization, penetration, and droplet diameter distribution) can be strongly correlated to injector operating conditions and injector geometric layout.

Focusing the attention on the injector geometric layout, one of the most interesting research field has regarded the injector hole shape influence on the Diesel spray characteristics. From this point of view, during the last years many Diesel injector manufacturing companies have switched from the classic cylindrical injector hole shape (Figure 1-a) to the so called *k-hole* layout (Figure 1-b) characterized by a progressively reduction of the hole cross-sectional area between inlet and outlet sections. The main spray characteristics distinguishing the *k-hole* to the *cylindrical-hole* can be summarized as follow:

- Improved spray stability thanks to the reduced cavitation intensity over the hole length
- Reduced spray cone angle
- Large jet penetration
- Reduced injection rate due to the reduced injector hole exit area

Because of the Diesel injector tendency in working under cavitating conditions (micro-orifices in conjunction to very high injection pressures), the correlation between the *k-hole* shape and cavitation evolution inside the hole itself attracted many research studies. Benajes et al. [10] and Payri et al. [11] performed experimental comparisons between cylindrical and conical nozzle holes finding, for the *k-hole*, a noticeable reduction of the injector cavitation tendency. Experimentally, it was underlined by the proportionality between the injector mass flow rate and the pressure drop over the injector operating field. The main reason of the different cavitation evolution between cylindrical and *k* holes was traced back to the capacity of the *k-hole* to promote the re-condensation of the vapour bubble eventually generated at hole entrance (flow detachment condition) before the hole outlet section. It helps to reduce the stochastic perturbation promoted on the liquid jet surface by the vapour bubble collapse and therefore to improve the spray stability.

A further evolution of the *k-hole* is represented by the *ks-hole* (from German "Konisch Strömungsoptimiert"). In the *ks-hole* the conical hole shape is associated to a huge rounded edge at hole entrance (Figure 1-c) obtained by a specifically designed hydro-grading (HG) process. The *ks-hole* design was studied to fulfill the following targets:

- To increase the pressure/velocity conversion efficiency [12]
- To reduce the vapor generation at hole entrance by a reduction of the flow separation
- To improve the *k-hole* benefit in reducing the Soot-NO_x trade-off and the coked matter adhesion [1]

Both *k-hole* and *ks-hole* are classified by the so called *k-factor* parameter defined as:

$$k - factor = \frac{d_{in} - d_{out}}{10} \tag{1}$$

where d_{in} and d_{out} are inlet and outlet hole diameters respectively. For automotive applications, the *k-factor* is usually bounded between 1.1 and 2.

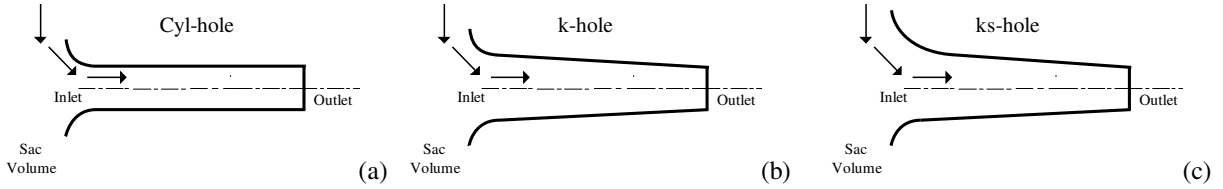

Fig. 1. Comparison between cylindrical (a), *k-hole* (b), and *ks-hole* (c) overall shapes.

2. Paper target and originality

The main motivation of the present work resides in the lack of data available in literature about the detailed comparison of the fluid dynamic performance characterizing the cylindrical, *k*, and *ks* injector hole geometries. To fill this lack, for each of the identified hole configuration a fully transient multiphase 3D-CFD simulation was performed in order to evaluate the holes fluid dynamic performances under identical operating conditions. All the considered hole geometries were installed on the same injector body.

As far as the structure of the paper is concerned, it is divided into three main sections. Firstly, the considered nozzle geometries are presented. Secondly, the adopted 3D-CFD simulation methodology is discussed in detail. Finally, the numerical results in terms of main fluid dynamic characteristics obtained for each injector are presented and compared each other.

3. Considered injector hole layouts

In Table 1 the main geometrical characteristics of the three considered hole layouts are compared. All the three injector holes were identically referred to the same Bosch CRIP-1 injector body characterized, in its standard configurations, by the data summarized in Table 2. The cylindrical hole geometric characteristics summarized in Table 1 corresponds to the base Bosch CRIP-1 injector hole layout. This Bosch injector was chosen because it was extensively studied by the authors [2,3,13], therefore its geometry, operating conditions, and fluid dynamic performances are well known.

About the *ks-hole* configuration considered in the present work, its real shape between the inlet/outlet sections was experimentally defined by the Werth Fiber Probe (WFP) machine. The WFP is mainly devoted to the measurements of extremely small geometries [14] thanks to the combined use of a probing element constituted by a glass-fiber with a melted spherical tip and an high-resolution CCD camera. During the measurement process the CCD camera captures picture sequences subsequently analyzed by an image processor to carry out the probe exact position [15]. In detail, for the *ks-hole*, three measurement sets (M_1, M_2, and M_3) were performed to evaluate its axial diameter evolution. Each measurement set started at the injector hole outlet section (injector axial coordinate equal to 0) and ended at the hole inlet section. Figure 2 shows the *ks-hole* diameter evolutions recorded by the M_1, M_2, and M_3 measurement sets. The authors refer to [16] for a complete description of the WFP machine and its application to the considered injector hole geometry.

Table 1. Injector hole geometric characteristics.

Hole layout		Cyindrical.*	k	ks
k-factor	[-]	0	1.3	1.3
Hole inlet diam.	[mm]	0.130	0.134	0.134
Hole outlet diam.	[mm]	0.130	0.121	0.121
Hole length	[mm]	0.75	0.75	0.75
Inlet radius	[µm]	~20	~20	~40

*Base injector hole layout for the Bosch CRIP-1 injector.

Table 2. Bosch CRIP-1 standard configuration.

Injector hole k-factor	[-]	0
Total number of injector hole	[-]	6
Working pressure range	[MPa]	14-16
Flow @ 10MPa	[cm^3/30s]	425*

*Without needle.

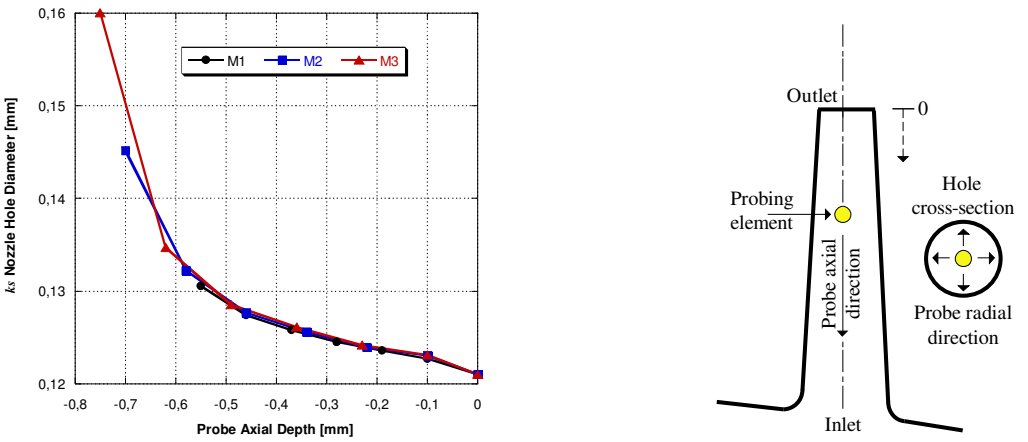

Fig. 2. Mean hole diameter evolutions recorded over the injector axis by the M1, M2, and M3 measurement sets.

4. Methodology of the analysis

All the simulations presented in this study were performed by using the Reynolds-averaged Navier-Stokes (RANS) simulation approach [17]. The commercial Fluent v12 CFD software was considered for the analysis [18]. Exploiting the injector body symmetry, only a sixth of the real fluid dynamic volume was considered (Figure 3-a).

To correctly reproduce the injector internal flow field, the CFD simulation methodology must satisfy two main criteria:

- A fully transient simulation methodology has to be adopted. Therefore, the needle motion must be reproduced during the simulation
- A specific multiphase approach has to be considered in order to simulate the liquid/vapor phase transition

In the next paragraphs these two aspects will be discussed.

4.1. Mesh motion technique

The initial mesh was generated at a needle lift equal to 5µm (simulation time equal to 0s). The domain was discretized by a fully unstructured hexahedral approach taking particular attention to the mesh structure close to the hole entrance (Figure 3-b).

Starting from the initial lift (5µm), during the simulation the needle was moved following the profile showed in Figure 4-a. To manage the change-in-shape of the computational domain the well-known layering approach was adopted [18]. On the basis of this method, the needle surface and the first four hexahedral layer attached to it were moved rigidly (Figure 4-b). This rigid motion produced the increment of the fifth cell layer height till a maximum value defined by the user. Over this maximum cell height value, an additional hexahedral cell layer was added just below the layering plane showed in Figure 4-b. During the needle closing phase the added cell layers were progressively collapsed to allow the needle to reach its initial position (5µm from the nozzle surface at seating zone). The choice to move the first four hexahedral cell layers attached to the needle surface rigidly together the needle itself was laid down the law to improve the near wall solution also on the needle moving wall.

On the basis of the mesh motion set-up, during the simulation the mesh size was ranging from ~300000 cells at needle initial position to ~380000 cells at needle maximum lift.

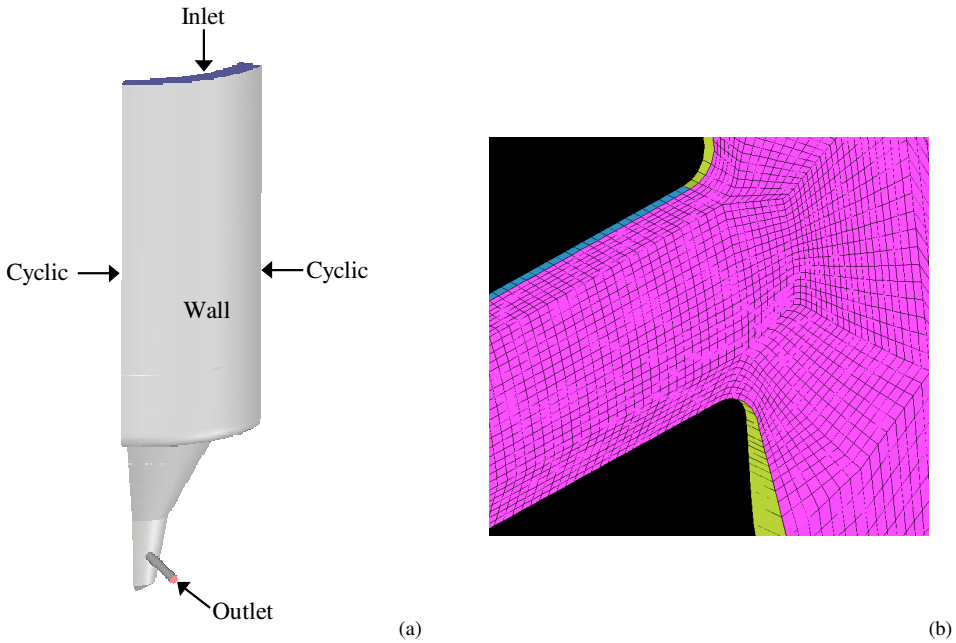

Fig. 3. Bosch CRIP-1 computational domain (a) and mesh structure close to the needle entrance (b).

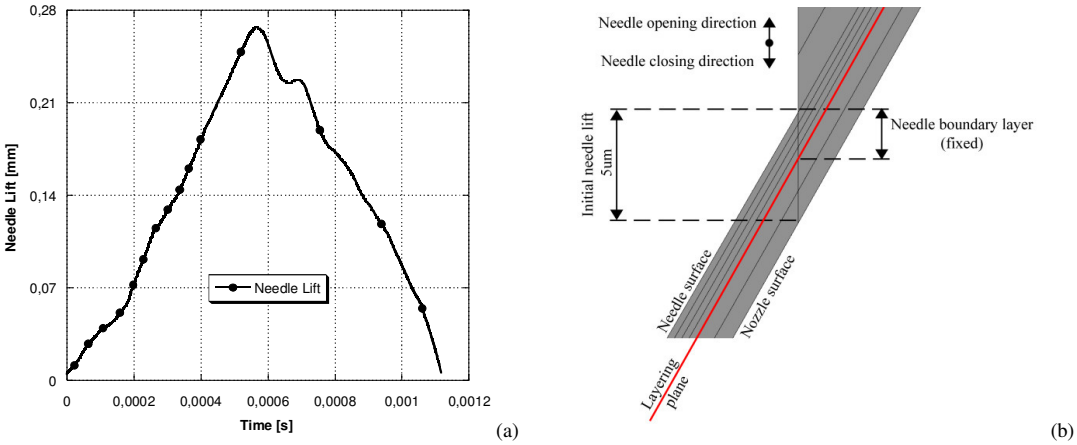

Fig. 4. Needle lift profile (a) and schematic representation of the layering mesh motion strategy (b).

4.2. Numerical set-up

All the multiphase simulations were performed adopting a first order implicit transient formulation and a fixed time step (1e-6s).

The VOF approach [18] was coupled to the Singhal *et al.* cavitation model [19,20] to manage the liquid/vapor transition. The Singhal cavitation model is based on the assumption of a perfect mixing between the liquid and the vapor phases and takes into account all first order effects of a multiphase flow as: phase change, bubble dynamics, turbulent pressure fluctuations, and non-condensable gases.

The flow-wall interaction was managed by the non-equilibrium wall function based on a law of the wall for mean velocity sensitized to pressure gradients [18].

To reproduce the turbulence effects on the mean flow the realizable k-ε turbulence model was considered [17].

Pressure, momentum, and volume fraction equations were discretized by using a second-order differencing schemes [17]. All the other equations were discretized adopting the first-order Up-Wind scheme [17].

4.3. Boundary conditions

All the three injector layouts considered in the present work were evaluated by imposing the same operating conditions summarized in Table 3.

On the inlet section a total pressure boundary condition was fixed while on the outlet hole section a static pressure value was imposed.

The working fluid was represented as a single-component fuel having the same overall physical properties of the ISO-4113 [19] characterized by a saturation pressure equal to 2370Pa at the considered fuel temperature. This phase-change pressure threshold was corrected during the simulation by the Singhal cavitation model to take into account the effect of the turbulence-induced pressure fluctuations [19].

The fuel temperature variation inside the injector was considered negligible. Therefore, the nozzle flow was considered as isothermal.

The initial values for the turbulent kinetic energy (k) and its dissipation rate (ε) at Inlet/Outlet boundaries were set on the basis of the following equations:

$$k = \frac{3}{2}(UI)^2 \tag{2}$$

$$\varepsilon = {C_\mu}^{3/4}\frac{k^{3/2}}{l} \tag{3}$$

The turbulent intensity I was set to 5% while the turbulent integral length scale l was set to the 7% of the inlet/outlet section characteristic length [17].

The operating conditions investigated by the CFD simulations are summarized in Table 3.

Table 3. Injector hole geometric characteristics.

Parameter		Quantity
Fuel	[-]	ISO-4113
Fuel temperature	[°C]	30
Injection pressure	[MPa]	20*
Outlet pressure	[MPa]	0*

* Relative to atmospheric pressure.

The multiphase simulation strategy presented in the previous pharagrahs was extensively validated against the experimental throttle-flow cases presented by Winklhofer *et al.* [22] concerning three quasi-2D geometries with the same length/thickness (1000µm/300µm) and different *k-factors*. For sake of brevity, the authors refer to [20] for a complete description of the simulation methodology validation.

5. Result analysis

The analysis of the cylindrical, *k-hole,* and *ks-hole* fluid dynamic performances were subdivided into two steps:

- Firstly, the three considered hole geometries were compared in terms of their main fluid dynamic performances as mass flow rate and mean velocity/turbulence data on the hole outlet sections.
- Secondly, the different cavitation evolutions recorded for the three considered layouts were analyzed and compared each other.

5.1. Cylindrical, k-hole, and ks nozzle flow fields

Figure 5-a shows the mean velocity profiles recorded at the hole outlet sections over the injection period. The hole layouts having a *k-factor* different from zero resulted characterized by the highest mean velocity value on the hole outlet section. It was mainly ascribed to the progressively reduction of the cross section area characterizing the *k* and *ks* holes respect to the cylindrical one. The flow velocity associated to the *ks-hole* was the higher because the HG process, specifically designed for it, allowed to improve the flow efficiency at hole entrance.

About the flow velocity difference observed between the cylindrical and the *k* holes on the nozzle outlet sections, it is important to underline how it was not representative of the real difference between their maximum flow velocities. In fact, for the cylindrical hole the maximum flow velocity magnitude was similar to the *k* holes but its value was reached at the "vena-contracta" section just downstream the hole entrance and not on the hole outlet section (Figure 6). At the same time, the effective flow area characterizing the cylindrical hole at the "vena-contracta" section was higher than the minimum flow area characterizing the *k* holes.

The final result emerging from the velocity and the effective flow area trends assured the highest mass flow rate to the cylindrical hole (Figure 5-b).

During the injection period, the jet turbulence level was monitored in terms of turbulent kinetic energy (TKE) and turbulence dissipation energy (TDE) on the hole outlet sections versus the needle lift. As showed in Figure 7, by considering a nozzle characterized by a *k-factor* different from zero the turbulence level was drastically reduced. It was the result of the increased flow uniformity at the hole outlet section associated to the conical shape.

From the spray point of view, the increased outlet flow velocity associated to the reduced turbulence level resulted for the *k* and *ks* holes in a reduction of the primary breakup capability and in a jet penetration enhancement [23]. In first instance, the authors correlated the primary break-up intensity to the hole geometries by the experimental results proposed by Sallam *et.al* [24,25]. Sallam performed experimental studies on the liquid turbulent jets in still air by which it was possible to extract useful correlation to evaluate the expected droplet Arithmetic Mean Diameter (D_{10}) and the Sauter Mean Diameter (SMD). Following the Sallam correlations, on the basis of the fluid dynamic averaged values at the hole outlet section (needle at full open position) the D_{10} and the SMD values reported in Table 4 were found.

Figures 8 and 9 show the vapor distribution recorded on the cylindrical and *ks-hole* surfaces during the injection process. As expected, passing from the cylindrical to the *ks-hole* the vapor generation along the hole axis was drastically reduced thanks to the tendency of the conical hole configuration to avoid the flow detachment at hole entrance and to promote the flow uniformity toward the hole outlet section. The reduction of the hole cavitation tendency recorded by the *k* and *ks* configurations helps to increase the spray stability and to reduce the cavitation erosion risk. On the other hand, also the reduction of the *k*/*ks* hole cavitation tendency is going toward a reduction of the overall turbulence level inside/outside the injector hole.

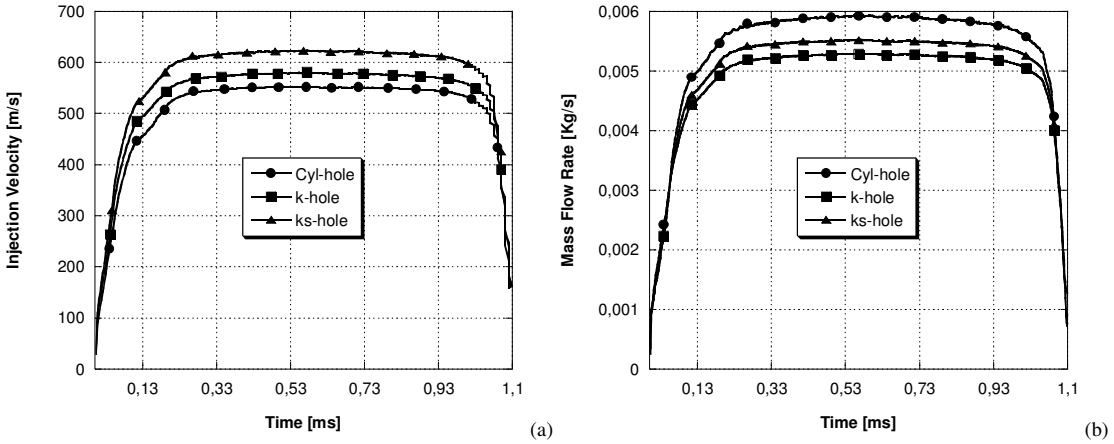

Fig. 5. Flow mean velocity (a) and mass flow rate (b) versus the injection time at hole outlet sections.

Fig. 6. Comparison between cylindrical (a) and *ks* (b) velocity distributions over the hole axial section at maximum needle lift.

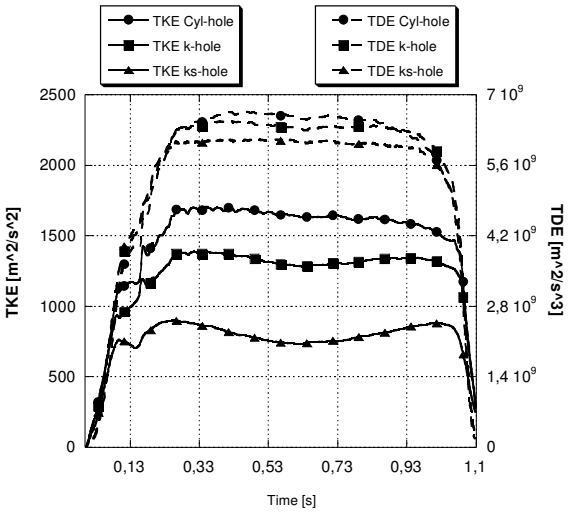

Fig. 7. TKE and TDE average values recorded on the considered nozzle outlet sections versus the injection time.

Table 4. D_{10} and SMD values extracted on the of the Sallam *et.al* [24,25] experimental correlations.

	D_{10} [µm]	SMD [µm]
Cylindrical	~5	~6
k	~10.7	~13.4
ks	~12.8	~16.0

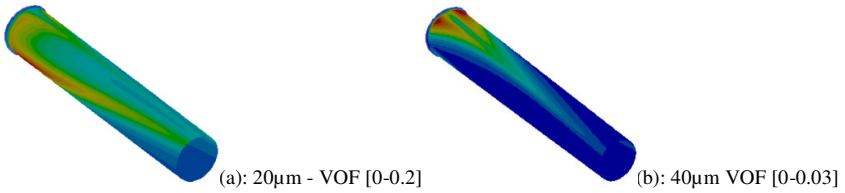

Fig. 8. Cavitation inception point for the cylindrical (a) and the *ks-hole* (b) geometries.

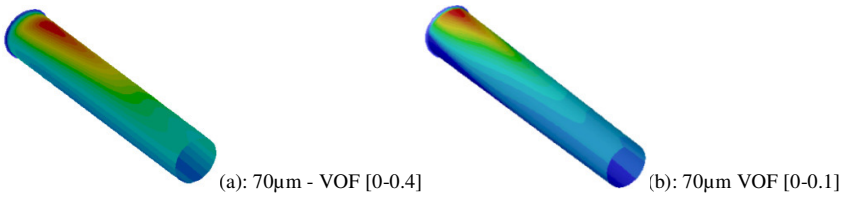

Fig. 9. Cavitation inception point for the cylindrical (a) and the *ks-hole* (b) geometries.

6. Conclusions

The main objects of the present work was the comparison of the fluid dynamic performances of three different Diesel nozzles: cylindrical, *k hole*, and *ks-hole*. To fulfill this goal a 3D-CFD fully transient multiphase approach was adopted. All the considered nozzle layouts were belonging to the same engine size. The simulation approach was previously validated against experimental results.

The *ks-hole* geometry was experimentally characterized by the use of the *WFP* machine. Thanks to the *WFP* machine it was possible to carry out the *ks-hole* real internal shape between inlet/outlet sections.

With respect to the cylindrical hole shape, the conical holes showed a quite evident reduction of the mass flow rate mainly linked to the reduction of the hole outlet section. However, thanks to the improved flow efficiency at inlet section, by the *ks-hole* geometry it was possible to limit the mass flow rate reduction observed for the *k* and *ks* holes. At the same time, the increased flow uniformity associated to the conical nozzle shapes on the outlet section resulted in a significant reduction of the flow turbulence level and therefore in a reduction of the expected primary breakup intensity.

About the cavitation evolution over the nozzle hole, for the *ks-hole* the vapor generation was completely suppressed over all the injection period. It was possible thanks to the improved fluid dynamic conditions at *ks-hole* entrance guaranteed by the huge rounding edge value.

In conclusion, the tested *ks-hole* guaranteed a very good fluid dynamic efficiency about the pressure-velocity conversion that helped to reduce the drawback effect of the conicity on the mass flow rate. At the same time, the *ks-hole* geometry allowed to suppress the vapor generation over the hole length with evident advantage about the cavitation erosion risk reduction. However, the improved conditions in terms of flow uniformity inside the *ks-hole* produced a significant reduction of the jet primary breakup intensity.

Reference

[1] Mahr B., Future and Potential of Diesel Injection Systems, THIESEL 2002 Conference on Thermo- and Fluid-Dynamic Processes in Diesel Engines.

[2] Bianchi G., Falfari S., Brusiani F., Pelloni P. et al., Numerical Investigation of Critical Issues in Multiple-Injection Strategy Operated by a New C.R. Fast-Actuation Solenoid Injector, SAE Technical Paper 2005-01-1236, 2005.

[3] Bianchi G., Falfari S., Brusiani F., Pelloni P. et al., Advanced Modelling of a New Diesel Fast Solenoid Injector and Comparison with Experiments, SAE TRANSACTIONS- JOURNAL OF ENGINES. vol. 113, pp. 1 - 14.

[4] Mulemane A., Han J., Lu P., Yoon S. et al., Modeling Dynamic Behavior of Diesel Fuel Injection Systems," SAE Technical Paper 2004-01-0536, 2004.

[5] Payri F., Margot X., Patouna S., Ravet F. et al., A CFD Study of the Effect of the Needle Movement on the Cavitation Pattern of Diesel Injectors, SAE Technical Paper 2009-24-0025, 2009.

[6] Som S., Aggarwal S., El-Hannouny E., and Longman D., Investigation of nozzle flow and cavitation characteristics in a diesel injector, Journal of Engineering for Gas Turbines and Power, vol. 132, no. 4, 2010.

[7] Nishida K., Zhang W., and Manabe T., Effects of Micro-Hole and Ultra-High Injection Pressure on Mixture Properties of D.I. Diesel Spray, SAE Technical Paper 2007-01-1890, 2007.

[8] Blessing M., König G., Krüger C., Michels U. et al., Analysis of Flow and Cavitation Phenomena in Diesel Injection Nozzles and Its Effects on Spray and Mixture Formation, SAE Technical Paper 2003-01-1358, 2003.

[9] Montanaro A., Allocca L., Ettorre D., Lucchini T., Brusiani F., Cazzoli G., Experimental Characterization of High-Pressure Impinging Sprays for CFD Modeling of GDI Engines, 2011-01-0685, SAE World Congress, Detroit, Michigan, USA, April 2011.

[10] Benajes J , Pastor J.V., Payri R., Plazas,A. H., Analysis of the Influence of Diesel Nozzle Geometry in the Injection Rate Characteristics, J. Fluids Eng 2004; 126:63–71.

[11] Payri R., Garcia J.M., Salvador F.J., Gimeno J., Using Spray Momentum Flux Measurements to Understand the Influence of Diesel Nozzle Geometry on Spray Characteristics, Fuel 2005; 84:551–61.

[12] He L. and Ruiz F., Effect of Cavitation on Flow and Turbulence in Plain Orifice for High-Speed Atomization, Atomization and Sprays, 1995. 5(6):pp. 569-584.

[13] Bianchi G. M., Falfari S., Brusiani F., Pelloni P., Osbat G., Parotto M., Di Gioia R., The Role of Simulation in the Development of a Fast-Actuation Solenoid C.R. Injector System, ICEF2004-847, ASME Internal Combustion Engine Division: 2004 Fall Technical Conference, Long Beach, California, USA, October 2004.

[14] Product Information. Giessen: Werth Messtechnik, 2004.

[15] Baltes H., Brand O., Fedder G.K., Hierold C., Korvink O., Tabata D., Microengineering of Metals and Ceramics: Part II, Editor(s): Detlef Löhe, Jürgen Haußelt, 2005.

[16] Brusiani F., Bianchi G. M., and Di Gioia R., Experimental Characterization of the Geometrical Shape of ks-hole and Comparison of its Fluid Dynamic Performance Respect to Cylindrical and k-hole Layouts, SAE International Journal of Engines 2013-24-0008, 2013.
[17] Versteeg H.K., Malalasekera W., An Introduction to Computational Fluid Dynamics: The Finite Volume Method (2nd edition), Longman, 2006.
[18] Fluent v12 User Manual, Fluent Inc.
[19] Singhal A. K., Li H. Y., Athavale M. M., and Jiang Y., Mathematical Basis and Validation of the Full Cavitation Model, ASME FEDSM'01, New Orleans, Louisiana, 2001.
[20] Brusiani F., Bianchi G.M., Negro S., Comparison of the Homogeneous Relaxation Model and a Rayleigh Plesset Cavitation Model in Predicting the Cavitating Flow Through Various Injector Hole Shapes, SAE Technical Paper 2013-01-1613, 2013.
[21] Mirosław Chorazewski M., Dergal F., Sawaya T., Mokbel I., Grolier J.P., Jose J., Thermophysical properties of Normafluid (ISO 4113) over wide pressure and temperature ranges, Fuel Volume 105 2013 440 – 450.
[22] Winklhofer E., Kull E., Kelz E., and Morozov A., Comprehensive hydraulic and flow field documentation in model throttle experiments under cavitation conditions, 17th Annual Conference on Liquid Atomization and Spray Systems, Zurich, Switzerland, September 2001.
[23] Som S., Ramirez A.I., Longman D.E., Aggarwal S.K., Kastengren A.L., El-Hannouny E.M., Effect of Nozzle Orifice Geometry on Spray, Combustion, and Emission Characteristics under Diesel Engine Conditions, Fuel 90 (2011) pp. 1267-1276.
[24] Sallam K. A., and Faeth G. M., Surface Properties During Primary Breakup of Turbulent Liquid Jets in Still Air, AIAA Journal, Vol. 41, No. 8, August, 2003.
[25] Brusiani F., Bianchi G. M., and Tiberi A., Primary Breakup Model for Turbulent Liquid Jet Based on Ligament Evolution, SAE Technical Paper 2012-01-0460, 2012.